# A Nanocrystal Sensor for Luminescence Detection of Cellular Forces

Charina L. Choi,[1,2]* Jonathan Chou,[3,4]* Katie M. Lutker,[1,2] Zena Werb,[3,4] A. Paul Alivisatos[1,2]†

[1]Material Sciences Division, Lawrence Berkeley National Laboratory, Berkeley, CA 94720

[2]Department of Chemistry, University of California, Berkeley, CA 94720

[3]Department of Anatomy, University of California, San Francisco, CA 94143

[4]Program in Biomedical Sciences, University of California, San Francisco, CA 94143

*These authors contributed equally to this work

†To whom correspondence should be addressed. E-mail: APAlivisatos@lbl.gov

# A Nanocrystal Sensor for Luminescence Detection of Cellular Forces

**Quantum dots have been used as bright fluorescent tags with high photostability to probe numerous biological systems. In this work we present the tetrapod quantum dot as a dynamic, next-generation nanocrystal probe that fluorescently reports cellular forces with spatial and temporal resolution. Its small size and colloidal state suggest that the tetrapod may be further developed as a tool to measure cellular forces in vivo and with macromolecular spatial resolution.**

Cell-generated forces on the surrounding extracellular matrix play a crucial role in important processes ranging from stem cell differentiation to cancer metastasis (*1-3*). These forces have been measured directly with spatial resolution (*4*) by quantifying cell-induced displacements in microfabricated arrays of fluorescent particles (*5*) and elastomeric vertical cantilevers (*6*). Such methods have yielded important insights into cell mechanical behavior and mechanotransduction (*4*). However, while cellular mechanics are ultimately generated by structures at the size scale of a single protein, current techniques cannot map forces with nanoscale spatial resolution. Furthermore, current techniques do not allow for in vivo measurements due to geometric restrictions. Here we demonstrate that the luminescence wavelength of a colloidal nanocrystal, the tetrapod quantum dot, shifts in response to cell-generated stresses. This result creates a path towards studies of cellular forces with nanoscale resolution and geometric flexibility.

The CdSe/CdS tetrapod nanocrystal consists of a zinc blende CdSe quantum dot core with four tetrahedrally protruding wurtzite CdS arms. The tetrapod has dimensions of 4 nm for

the core and arm diameters and 15-50 nm for the arm length. Like its spherical quantum dot predecessor, the CdSe/CdS tetrapod exhibits bright and narrow photoluminescence, with a Gaussian-shaped ensemble emission spectrum. Previous work showed that the peak emission wavelength of the tetrapod shifts as a function of applied stress (*7, 8*) and is sensitive to perturbations on the nanonewton (nN) scale (*9*). Because cell-generated forces are also on the order of nanonewtons (*4*), we postulated that tetrapods might be able to sense and fluorescently report cellular mechanical stresses.

To investigate this idea, we designed a luminescent tetrapod array on which cells could be cultured (**Fig. 1a, Supplementary Fig. 1**), using tetrapods of 25 nm arm length. An ensemble of these tetrapods exhibits luminescence peak emission at 1.94 eV with a peak full-width-half-maximum of 0.09 eV. As-synthesized tetrapods are not water soluble, so we first made them biocompatible using an amphiphilic polymer wrapping technique (*10*). The resultant carboxylate-functionalized tetrapods were covalently attached to an amine-functionalized transparent substrate via amide bond formation chemistry, achieving a tetrapod monolayer array (**Supplementary Fig. 1**). We chose to culture HL-1 rat cardiomyocytes, which exhibit spontaneous and periodic contractions in vitro, on top of a tetrapod monolayer to apply periodic stresses to the luminescent array (**Fig. 1b, Supplementary Video 1, Supplementary Video 2**, (*11*)). The morphological and contractile phenotype of the cells was similar to those grown in culture without the tetrapod monolayer.

To determine whether cell contractions could switch the luminescence emitted by the tetrapod array, we built an acousto-optic tunable filter (AOTF) microscope to collect spatially resolved luminescence spectra of the array in real time (**Supplementary Fig. 2**). The AOTF microscope (*12*) images the intensity of light emitted by the sample as a function of band pass.

Images taken at multiple band pass frequencies are stacked together to create a map with spectral data at each image pixel. Luminescence spectra of the tetrapod array were collected by imaging the emission intensity of the array at 100 band pass frequencies ranging from 1.81-2.14 eV. We collected 324 spectra simultaneously in 350 ms over a total area of 18 x 18 pixels with a pixel resolution of 5.1 $\mu m^2$. Each spectrum was fit to a Gaussian curve, and the emission peak energy at each pixel was used to create a spectral map. Twenty successive spectral maps were imaged for a given spot to observe luminescence behavior over time.

We observed clear time-dependent color shifts in the tetrapod array emission due to cardiomyocyte contractions (**Fig. 1c, Supplementary Fig. 3**). Fluorescence red shifts relative to a control array were observed, indicating a breaking of tetrahedral symmetry in the nanocrystals induced by cell beating. Utilizing results from electronic structure modeling of uniaxially compressed tetrapods (*9*), we calculate an average shift-inducing force of 0.7 ± 0.4 nN per tetrapod. This range of values is consistent with previous measurements of contractile forces from cardiomyocytes (*5*). Although the measured force behavior is likely altered relative to physiologic mechanics due to the stiff and two-dimensional culture substrate, the experimental geometry provides a simple system to probe nanocrystal fluorescence in response to cell-generated stresses. Importantly, the observed emission shifts demonstrate that tetrapods can sense cellular forces and respond with luminescent readout.

The small size and colloidal nature of the tetrapod allow its further development towards imaging cellular stresses with macromolecular spatial resolution and in a variety of biological geometries. Cellular forces are generated by cytoskeletal proteins such as microtubules and actin filaments, and are localized to subcellular structures such as focal adhesions. Nanoscale resolution will allow quantitative investigations of how stresses are sensed and relayed at single

protein complexes consisting of integrin clusters to the cytoskeleton. Furthermore, colloidal particles can be treated as a chemical reagent, enabling use of the tetrapods to study processes that occur on flat surfaces, as shown in the present work, in three-dimensional matrices, or even within tissues or between cells. The key to measurements in more complex geometries will be careful anchoring of the nanocrystal through smart surface functionalization for maximal tetrapod deformation by the stress of interest.

Because the tetrapod responds optically to cell-generated stresses, it can also be used to convert biochemical inputs into optical signals, which may be useful in a synthetic biology circuit, for example. Future work will enable fully quantitative force measurements through a detailed characterization of the tetrapod response to biologically relevant stress states and more physiologic studies of cell mechanics by attachment of tetrapods within softer extracellular matrix-like materials. These studies will provide an important complement to measurements of in vitro cellular stress and tension (*4, 13*), inter-macromolecular forces (*14*), and extracellular matrix strain (*15*).

**Acknowledgements**

We gratefully acknowledge Arron Campi and John Kump (Crystal Technology, LLC) and Dale Gifford (Impact Zone) for AOTF and PCB design. We also thank Andrew Olson for synthesis of CdSe/CdS tetrapods, Sarah Swisher and Jesse Engel for electronics assistance, Joseph Shieh for providing HL-1 cells, and Dan Fletcher, Marc Shuman, and Philip Jess for helpful discussions. Work on AOTF microscope construction was supported by the Physical Chemistry of Semiconductor Nanocrystals Program, KC3105, Director, Office of Science, Office of Basic Energy Sciences, of the United States Department of Energy under Contract No. DE-AC02-05CH11231. Work on spectral imaging and analysis was supported by the National Institutes of Health through a pilot project of the Bay Area Physical Sciences Oncology Center, U54 CA143836. Work on tetrapod array fabrication was supported by the Dauben Fellowship (CLC). Work on cardiomyocyte culture was supported by a Department of Defense predoctoral fellowship, W81XWH-10-1-0168 (JC) and by funds from the National Institutes of Health U01 ES019458.

**Figure 1.** Beating cardiomyocytes induce shifts in the fluorescence color of a luminescent tetrapod nanocrystal array. **(a**) Schematic of a cell grown on a fibronectin-coated monolayer of tetrapod nanocrystals. (**b**) HL-1 cells grow and beat on a tetrapod substrate. Synchronized contractions are exhibited over the entire area (**Supplementary Video 1**). Yellow lines highlight one area that contracts (right) and relaxes (left). (**c**) Spectral map snapshots of peak shifts from a cardiomyocyte-perturbed tetrapod array over time. Snapshots are taken from the area of tetrapods directly below the area shown in **b**. The change in peak energy at each pixel is plotted relative to a standard spectral map containing the highest peak energies observed; each frame represents 350 ms spectral integration time. Side length in **b** and **c** is 40.7 μm.

**References**


1. V. Vogel, M. P. Sheetz, *Curr. Opin. Cell. Biol.* **21**, 38 (2009).
2. D. T. Butcher, T. Alliston, V. M. Weaver, *Nat. Rev. Cancer* **9**, 108 (2009).
3. A. J. Engler *et al.*, *J. Cell. Biol.* **166**, 877 (2004).
4. C. S. Chen, J. Tan, J. Tien, *Annu. Rev. Biomed. Eng.* **6**, 275 (2004).
5. N. Q. Balaban *et al.*, *Nat. Cell Biol.* **3**, 466 (2001).
6. J. L. Tan, J. Tien, D. Pirone, D. S. Gray, C. S. Chen, *Proc. Natl. Acad. Sci. USA* **100**, 1484 (2003).
7. C. L. Choi, K. J. Koski, S. Sivasankar, A. P. Alivisatos, *Nano Lett.* **9**, 3544 (2009).
8. C. L. Choi, K. J. Koski, A. C. K. Olson, A. P. Alivisatos, *Proc. Natl. Acad. Sci. USA* **107**, 21306 (2010).
9. J. Schrier, B. Lee, L. W. Wang, *J. Nanosci. Nanotechnol.* **8**, 1994 (2008).
10. T. Pellegrino *et al.*, *Nano Lett.* **4**, 703 (2004).
11. W. C. Claycomb *et al.*, *Proc. Natl. Acad. Sci. USA* **95**, 2979 (1998).
12. E. S. Wachman, W. Niu, D. L. Farkas, *Biophys. J.* **73**, 1215 (1997).
13. W. R. Legant *et al.*, *Nat. Methods* **7**, 969 (2010).
14. M. Streichfuss *et al.*, *Nano Lett.* **11**, 3676 (2011).
15. J. W. Stone, P. N. Sisco, E. C. Goldsmith, S. C. Baxter, C. J. Murphy, *Nano Lett.* **7**, 116 (2007).

**Supplementary Information** for A Nanocrystal Sensor for Luminescence Detection of Cellular Forces

## Materials and Methods

*HL-1 cell culture on luminescent tetrapod substrates.* CdSe/CdS tetrapods were synthesized following previously reported methods (*1*). A polymer-wrapping procedure was used to water-solubilize the tetrapods and create carboxylic acid groups on the tetrapod surface (*2*). Tetrapod monolayer substrates (**Supplementary Fig. 1**) were fabricated by covalently linking the tetrapods to transparent coverglass slides (no. 1.0) functionalized with a dense amine surface (custom made SuperAmine slides, ArrayIt) via a 1-Ethyl-3-[3-dimethylaminopropyl]carbodiimide hydrochloride (EDC)/*N*-hydroxysulfosuccinimide (Sulfo-NHS) coupling reaction. CdSe/CdS tetrapods (4.5E-8 M in PBS buffer), EDC (0.24 mg, Sigma), and sulfo-NHS (0.66 mg, Pierce) were reacted overnight with the amine-coated coverglass to achieve monolayer coverage. Each slide was washed thoroughly with PBS buffer to ensure that only covalently bound tetrapods remained.

Tetrapod monolayer substrates were placed inside cell culture wells, and HL-1 cells were cultured on the tetrapod monolayer according to culture conditions previously described (*3*). Briefly, the nanocrystal substrate was first coated with a dilute solution of fibronectin (Sigma) for 1-2 hours. HL-1 cells were grown in Claycomb media (Sigma) supplemented with norepinephrine (100 μM), FBS (10%), L-glutamine (4 mM), and penicillin/streptomycin. The cells were plated onto the nanocrystal monolayer and

allowed to adhere overnight. One to two days later, the medium was changed, supplemented with HEPES buffer (25 mM), and the cells were imaged. HL-1 cells cultured on fibronectin-coated tetrapod substrates exhibited qualitatively similar morphological and contractile phenotypes as those grown on normal tissue culture plates.

*Acousto-optic tunable filter (AOTF) microscope.* A schematic of the microscope is shown in **Supplementary Fig. 2**. Our design is based on previous work utilizing an AOTF for spatially resolved spectral imaging (*4, 5*). Our samples were excited at 2.54 eV with an $Ar^+$ laser (3 mW total power, 300 μm spot size). Luminescence from the sample is collected through an objective (Zeiss 40x LD Plan-Neofluar, NA = 0.6 with correction collar) and this light is collimated using achromatic doublet lenses and sent through the AOTF (97-02838-01, Crystal Technology, LLC). An iris is used to block the undeflected beam, and the deflected beam is focused using an additional achromatic doublet lens onto a CCD (Andor iXon 897).

The computer sets 1000 radio frequencies (RFs) to be applied by the direct digital synthesizer (DDS) onto the AOTF. We calibrated the AOTF and found that $x_{eV} = .0205*(x_{MHz} – 91.41) + 1.942$, where $x_{MHz}$ = the applied RF (MHz) and $x_{eV}$ = the light frequency allowed to deflect through the crystal (eV). Typically, we applied a sweep of 100 different frequencies ranging from 85-101 MHz, which corresponds to 1.81-2.14 eV. The CCD collects an intensity image at each RF frequency with a total time (including exposure time and transfer time) of 3.5 ms per frequency, for a total spectral collection time of 350 ms. We used a custom made printed circuit board (PCB, Impact Zone) to synchronize the AOTF and CCD; the time offset between the two was 10 ns.

*Spectral data collection and analysis.* Samples were taken from a 37° C incubator and imaged on our microscope at room temperature. HL-1 cells exhibited beating on the tetrapod substrate throughout data collection. At each spot imaged, a brightfield movie (25 s, 10 frames per s), brightfield image (9.2 ms exposure time), and fluorescence image (9.2 ms exposure time) were collected using a camera (PaxCam 2+, MIS, Inc.) mounted on top of the microscope. Emitted light from the tetrapods was then sent through the AOTF to obtain spatially resolved photoluminescence spectra of the substrate (20 spectra at each pixel simultaneously, 350 ms total integration time per spectra). A brightfield movie was taken after spectra collection to determine whether any perturbations to cardiomyocyte contractions had been induced by laser excitation. In all spots studied, no changes in beating behavior following laser excitation were observed.

The time resolution for spectral collection was limited to 350 ms total integration time by the luminescence intensity reaching the CCD. Although the rate of cardiomyocyte beating was ~0.5-1 Hz, we were unable to consistently optimally capture in succession the stress changes within one beat cycle due to the rapid timescale of contraction (~100 ms) and variations in beating periodicity (**Supplementary Videos 1-2**). Future work will increase spatial and temporal resolution via improvements to tetrapod quantum yield and microscope design. Use of electrical stimuli and addition of a microscope stage with temperature and $CO_2$ control may further optimize sub-cycle stress imaging through synchronization of beating with spectral measurements and a more consistent beat frequency.

Spectral maps of shifts in peak emission were plotted to highlight changes in array luminescence (**Fig. 1c** and **Supplementary Fig. 3**). The change in energy at each pixel is calculated relative to a standard spectral map for a given area containing the highest peak energies observed at each pixel. A per pixel offset calculation is required since emission from the AOTF deflected beam was slightly spatially dispersed. The highest peak energies emitted by cardiomyocyte-perturbed array areas correspond to the average frequency emitted by an unperturbed control array, suggesting that the highest energies observed in a perturbed array represent a relatively unstressed state. This observation strongly advocates that cell-generated forces red shift tetrapod luminescence in the experimental geometry, in concordance with previous calculations (*6*) and demonstrations (*7, 8*) that symmetry-breaking deformations induce red shifting of the tetrapod energy gap.

To calculate the average force, the average and standard deviation in offset value over all pixels in a given area (6480 total, from 324 pixels per frame and 20 frames) were calculated and converted from MHz to eV using our determined calibration and eV to nN following previous electronic structure calculations (*6*). The force values reported in the main text were calculated using data from the area depicted in **Fig. 1b-c** and **Supplementary Fig. 3a**. An identical calculation on data from a control area (depicted in **Supplementary Fig. 3c**) determined an average force of 0.3 ± 0.2 nN, suggesting the minimum threshold of force detectable in our system. Work to thoroughly characterize the luminescence response of tetrapods to a set of all relevant stress states will provide an experimental eV to nN conversion, enabling more precise quantitative measurements of cell-generated forces.

**Supplementary Figure 1**. Fabrication of luminescent tetrapod substrates. (**a**) Fluorescence image of a CdSe/CdS tetrapod monolayer substrate upon excitation with a 2.54 eV $Ar^+$ laser. Scale bar, 100 μm. (**b**) As-synthesized CdSe/CdS tetrapod nanocrystals are surface-functionalized with phosphonic acid ligands (left); a schematic of a single ligand is shown for clarity. Following an amphiphilic polymer wrapping procedure the tetrapods are water soluble, with exposed carboxylic acid functional groups (center). The tetrapods are covalently linked to a transparent amine-functionalized coverglass substrate utilizing 1-Ethyl-3-[3-dimethylaminopropyl]carbodiimide hydrochloride (EDC)/*N*-hydroxysulfosuccinimide (Sulfo-NHS) coupling chemistry. Incubation of the coupling reaction followed by thorough washing of the substrate results in a tetrapod nanocrystal monolayer covalently attached to the coverglass surface.

**Supplementary Figure 2.** Diagram of the AOTF microscope used to collect photoluminescence spectra of a two-dimensional tetrapod array with spatial and temporal resolution.

**Supplementary Figure 3.** Beating heart cells induce shifts in the luminescence color emitted by a tetrapod array. (**a**)-(**b**) Snapshots of the change in peak emission over time of a fibronectin-coated tetrapod array periodically stressed by cardiomyocyte contractions. **a**-**b** exhibit different areas on the luminescent array; data in **a** is from the same area shown in **Fig. 1b-c**. (**c**) Snapshots of the change in peak emission over time of a fibronectin-coated tetrapod array without cardiomyocytes. **a-c** show ten successively

collected frames with a spectral integration time of 350 ms each. The change in peak energy at each pixel is plotted relative to a standard spectral map containing the highest peak energies observed. The side length of each frame is 40.7 μm.

**Supplementary Video 1.** HL-1 cells beating on a fibronectin-coated tetrapod array in the area featured in **Fig. 1b-c**.

**Supplementary Video 2.** HL-1 cell contractions on a fibronectin-coated array. The movie is centered on the cells featured in **Supplementary Video 1** but exhibits the substrate over a larger field of view.

**References**


1. A. Fiore *et al.*, *J. Am. Chem. Soc.* **131**, 2274 (2009).
2. T. Pellegrino *et al.*, *Nano Lett.* **4**, 703 (2004).
3. W. C. Clayclomb *et al.*, *Proc. Natl. Acad. Sci. USA* **95**, 2979 (1998).
4. E. S. Wachman, W. Niu, D. L. Farkas, *Biophys. J.* **73**, 1215 (1997).
5. N. Gupta, *Methods in Molecular Biology: Biosensors and Biodetection* **503**, 293 (1999).
6. J. Schrier, B. Lee, L. W. Wang, *J. Nanosci. Nanotechnol.* **8**, 1994 (2008).
7. C. L. Choi, K. J. Koski, S. Sivasankar, A. P. Alivisatos, *Nano Lett.* **9**, 3544 (2009).
8. C. L. Choi, K. J. Koski, A. C. K. Olson, A. P. Alivisatos, *Proc. Natl. Acad. Sci. USA* **107**, 21306 (2010).

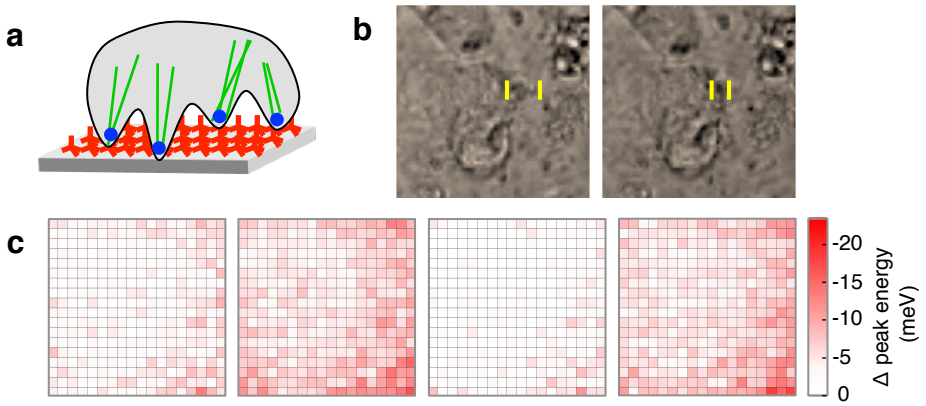


**Figure 1.**

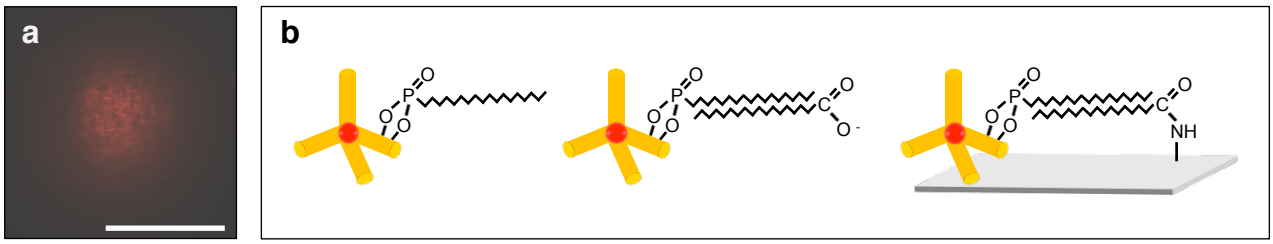


**Supplementary Figure 1.**

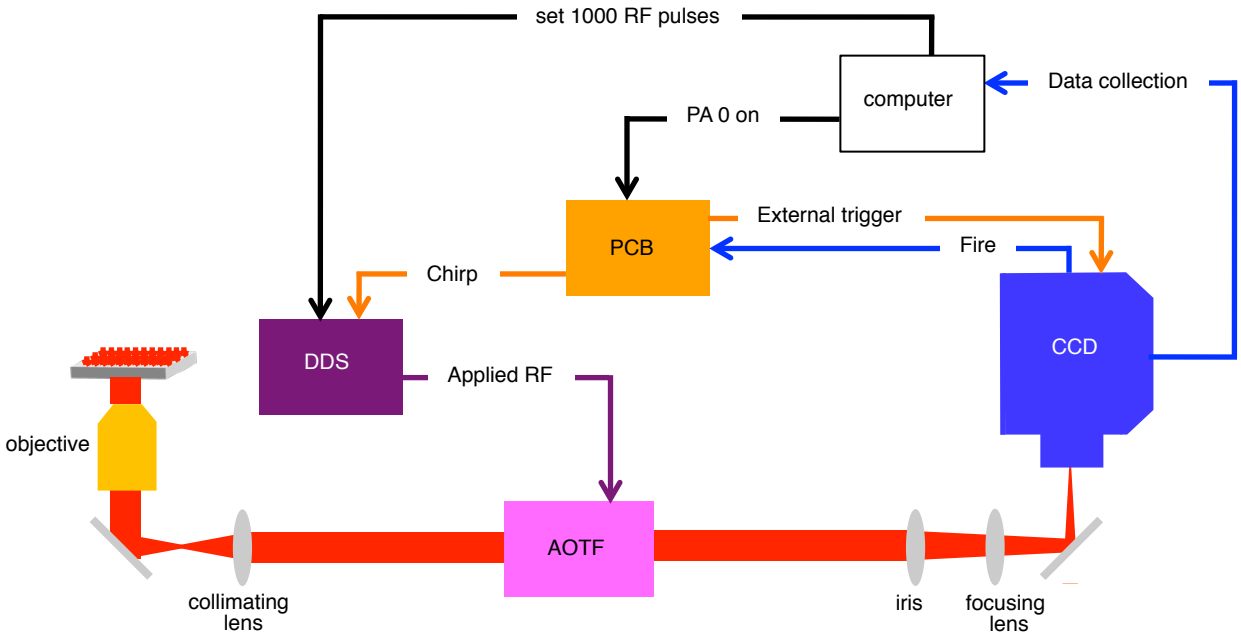


**Supplementary Figure 2.**

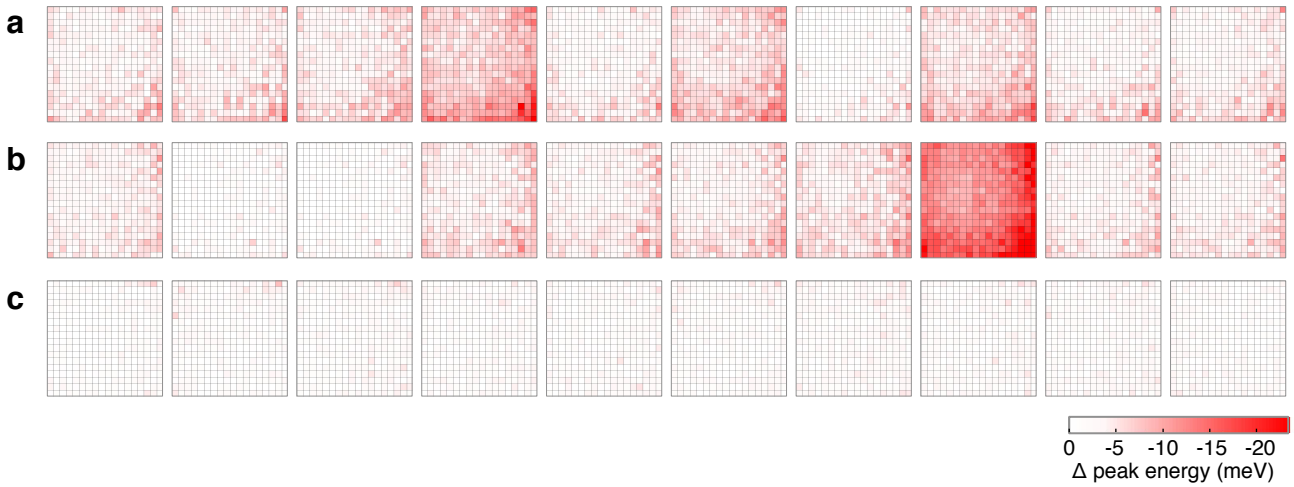


**Supplementary Figure 3.**